

# INTEGRATED RES WITH ANN-MPPT FOR EFFICIENT POWER GENERATION AND WIRELESS TRANSMISSION FOR PV APPLICATIONS

Mrs. K. Yojana  
Assoc Professor, ECE  
SBIT, KHAMMAM  
Email: [yojanak5@gmail.com](mailto:yojanak5@gmail.com)

Mrs. Bhavani  
Asst Professor, ECE  
SBIT, KHAMMAM  
Email: [bhavani1142@gmail.com](mailto:bhavani1142@gmail.com)

Ms. K. Sunitha  
Asst Professor, ECE  
SBIT, KHAMMAM  
Email: [sunitha.sunitha250@gmail.com](mailto:sunitha.sunitha250@gmail.com)

**Abstract-** The integration of renewable energy sources (RESs) into distribution power networks is of utmost importance due to the growing worldwide demand for energy and the pressing need to adopt more sustainable practices. An important part of building-integrated centralized generation in low-voltage (LV) DC networks is the usage of rooftop photovoltaic (PV) systems, which are the primary emphasis of this project. To maximize the efficiency of power production, a method called Maximum Power Point Tracking (MPPT) is used. This technique is based on Artificial Neural Networks (ANNs). It works especially well in partly shadowed situations, allowing the PV panels to harvest the most power possible. A Luo converter is used to monitor and optimize the power output of the PV system after it has produced electricity. Then, in order to transmit power wirelessly, the Luo converter's output is sent to a high-frequency converter. The ability to transmit electricity wirelessly improves the system's scalability and flexibility by removing the necessity for physical connections during energy transfer. An isolation transformer is linked to the output of the high-frequency converter to guarantee the system's safety and dependability. The high-frequency converter is protected from electrical risks and kept apart from components downstream by the isolation transformer. Lastly, DC loads are provided with the transformer's isolated output, which is then directed towards an electric vehicle (EV) battery. Lastly, a set of numerical simulations will be run using the MATLAB 2021a/Simulink program to verify the suggested controls.

## 1. INTRODUCTION

In the last ten years, there has been a meteoric rise in the number of studies focusing on photovoltaic (PV) systems. Solar photovoltaic (PV) array output power maximum power point tracking (MPPT) is essential for efficiency enhancement. When compared to methods based on artificial intelligence, conventional MPPT approaches perform worse, particularly in situations when there is partial shade or when the ambient circumstances are changing quickly, despite the fact that they provide a simpler framework and execution. Renewable energy supplies are the focus of intense study due to rising environmental concerns and the dread of fossil fuel depletion. Photovoltaic (PV) energy stands out among the many renewable energy sources. There is a strong foundation of benefits, including the ability to directly convert to electric power, minimum operating cost, and decreased pollutants. It is therefore not surprising that PV-based systems have become so prevalent in the energy industry. Despite PV systems' many benefits, one big drawback is the non-linear environmental dependence of their features. Improving the total system efficiency requires monitoring the highest power point of PV arrays. The integration of large-scale renewable distributed generating, enhanced communication and control techniques, and higher storage capacity are examples of how sophisticated technologies are reshaping power production and distribution networks. The static construction, small size, and low maintenance cost of solar PV (Photovoltaic) based energy producing systems make them a popular choice among renewable resources. However, PV systems often have a minimum output voltage, which impacts their efficiency and dependability.

With the minimum PV voltage being lower than the utility grid voltage, a high switching frequency device is required to raise it to grid voltage level. To do this, a DC/DC converter is integrated into the PV panel; this increases the voltage of the PV panel and therefore the efficiency of energy extraction.

### 1.1 STANDARD TESTING CONDITION OF SOLAR PV MODULE

The electrical output of a photovoltaic (PV) panel is specified to be 1000W/m<sup>2</sup> in a functioning cell operating at 25 °C with a significant air mass of 1.5, as per the industry Standard Test Conditions (STC). The irradiation level in Tamil Nadu is seen in Figure 1.2.



Figure: 1.1 Irradiance level in TamilNadu

Multiple photovoltaic cells are linked in series to form a PV module, which in turn produces the desired voltage. Typically, 36 or 72 cells are linked in series to create a perfect PV module. The PV modules are then linked in parallel to provide an increase in the array's current and voltage ratings, which are necessary to satisfy the load demand. To satisfy the electrical demand, the PV arrays, which produce electricity, need to be managed and, on occasion, adjusted. Commercially available PV modules provide unregulated DC output. The environmental factors could affect the PV array's output. The PV array's output may be adjusted with the use of power controllers, such as maximum power point trackers (MPPT). The MPPT optimizes the array's output while keeping the operating voltage constant at a given value. You may feed a DC load using this output. Use of inverters is necessary when dealing with AC loads, such as utility grid power, AC motors, etc. To get the most of the sun's rays, PV modules should be angled such that they face directly towards the sun. Reasons for this include solar radiation's direct beam component reflection on the panel's surface, a much higher incidence angle, and a line perpendicular to the surface and the beam's angle with the surface being more than 60°. By lowering the incidence angle, tracking panels that follow the sun's movement improve the amount of usable solar radiation. If tracking is not an option, a nice, all-year-round solution is to put the panels at a horizontal angle equal to the site latitude, facing solar south (when the panels are located in the Northern Hemisphere). On the other hand, the ideal tilt angle changes from season to season depending on the sun's angular location at midday or the turndown.

How much of an impact irradiance has on a solar array's efficiency is determined by the module technology. All the modules are defined by the rated parameters. One such metric that shows how the modules or their execution performs in low light is the maximum power voltage. This is a crucial factor to think about when the solar array is situated in a typical overcast scenario and the irradiance levels are lower than the STC. The temperature of the operational cells is influenced by factors like as the panel mount, insolation, ambient temperature, wind speed and direction, and module execution.

## 2.LITERATURE SURVEY

**Weiyang Zhou et al [2022]** In order to reduce the voltage seeking range for PV arrays operating under GLBC, a simple and quick voltage-location global MPPT (VL-GMPPT) approach has been suggested. To accomplish this, a GLBC-based mathematical model of the global maximum power point (GMPP) of a PV array is constructed. After that, the VL-GMPPT technique uses the IncCond approach to precisely locate the GMPP and a voltage-location mechanism to immediately relocate the operating point to the area around the GMPP. The suggested GMPPT approach is validated by displaying the results of both experiments and simulations. It was discovered that the suggested approach may cut down on tracking time by 90% compared to the traditional global searching strategy.

**Aranzazu D. Martin et al [2020]** suggested a WPSS and a WCC, which stand for wireless smart photovoltaic systems. Utilizing a WSN that is based on IEEE 802.15.4 technology in beacon enable mode and with a guaranteed time slot manages the sensing, coordination, and control data. Two essential components of any wireless PV monitoring system—data transfer and synchronous acquisition—are guaranteed by this. Every

photovoltaic module has its own independent, small, and inexpensive sensor node that transmits data to a central coordinator node. The sensor node's power usage is a meager 0.25 percent of the total power output from the solar module. The reference settings for each PV module are derived via a back-stepping controller that tracks the Maximum Power Point (MPP) using a buck-boost converter. The wireless solution ensures consistent controller performance and real-time monitoring via the use of low latency approaches. All of the network nodes can be easily identified by the centralized control, which greatly simplifies maintenance operations. Through experimental validation, we can see that the proposed wireless sensor system is secure and resistant to interference, and we can verify that it can monitor the maximum power transfer in a variety of weather conditions, with an MPPT efficiency of more than 99%.

**Xujian Shu et al [2022]** A significant problem for the current wireless power transfer (WPT) system using many repeaters is to suggest a power transfer while maintaining transfer efficiency close to unity at different transfer distances. This article offers a new WPT technique with many repeaters that is based on the idea of parity-time symmetry to solve the issue. The WPT relay system's coupled-mode model must first be defined. After that, we look examine the suggested WPT system's steady-state transfer properties with both an odd and an even number of repeaters. Based on the theoretical analysis, the suggested system maintains a constant output power and transfer efficiency regardless of the number of repeaters inserted between the transmitting and receiving coils. This is achieved automatically, without the need for tuning or feedback, up to a certain distance, regardless of whether the number of repeaters is odd or even. Proof of the theoretical analysis's validity is achieved by implementing the prototype with one and two repeaters.

**Huanjie Zhu et al [2020]** proposes a novel method of controlling the main side alone and a DC-DC converter for the front end to build a parity-time (PT) symmetrical WPT system that is series-series compensated. The technique consists of power closed-loop control, PT-symmetric online load detection, and negative resistance control of PT-symmetric circuits. We may potentially simplify the control method, boost the system's resilience, decrease the volume of the secondary side, and eliminate the demand for dual-side wireless communication and the secondary-side control circuit—all without the mutual inductance information. No matter the coupling coefficient or load, the proposed approach of managing just the main side of the system automatically stabilizes the output power at specified levels. The experimental data obtained from a prototype may be seen here.

**Fandan Zhao et al [2022]** The author suggests a high-power electric vehicle (EV) dynamic wireless power transfer (DWPT) system that uses a bipolar nonsalient pole (BNSP) transmitter design borrowed from motor theory. The current I-type, S-type, and N-type transmitters used in DWPT applications are categorized as bipolar salient pole (BSP) transmitters, providing a benchmark for investigating and assessing BNSP transmitters in terms of concept, characteristics, and performance. There is a comparison of BNSP and BSP transmitters, including their design specifications and additional criteria. Comparisons between the magnetic and finite-element models of BNSP and BSP transmitters allow for the analysis of coupling flux and leakage flux of the former. We study and evaluate the coupling performance of BNSP and BSP transmitters in simulation based on their modular architecture and how it is affected by the module gap in real-world applications. Contrast trials corroborate all of the theoretical conclusions.

**Jialong Qu et al [2020]** provide an innovative way to tap into the energy surrounding a 110-kV transmission line's magnetic field and send it to the transmission tower's online monitoring gear over an insulating distance of 1.1 meters. The composite insulation material that forms the first high-voltage insulator with wireless power transfer (WPT) capabilities is applied to printed circuit board resonators. The stringent HV tests at 550 kV were passed by the prototype of the HV insulator. Analyzed and confirmed by experimental results is the WPT property of the HV insulator, which takes into account the influence of corona rings.

**Lihao Wu et al [2020]** argues that wireless power transfer (WPT) might be a reliable, easy, and sensible way to charge electric vehicles. Still preventing wireless charging technology for EVs from reaching the market is the challenge of achieving high power and efficiency with a wide misalignment tolerance. Our solution to these issues is a novel WPT design based on PT principles that employs a large number of decoupled receiving coils. This PT-based WPT system's circuit model is ready to go. Theoretically, we discover that the transfer efficiency and output power of the proposed system remain constant throughout a wide range of coupling coefficient values. Notably, in comparison to the conventional WPT system that relies on a single receiving coil, an array of coils may improve transfer efficiency while simultaneously reducing system stress. The suggested WPT system is evaluated by building and testing a 1-kW laboratory prototype.

**Xiaoyang Tian et al [2022]** calculates the optimal omnidirectional WPT using an algorithm that accounts for scattered transmitter coils. Examples of real-world WPT applications that endanger people include wireless rechargeable medical implants and common household appliances; the suggested method may minimize exposure to radiofrequency electromagnetic radiation while simultaneously achieving the quickest charging time. The current gold standard is based on the magnetic intensity calculations of the multicoupling

WPT systems; we provide a more tractable model of the magnetic threshold and compare it to it. We accomplish maximum power tracking and flux suppression at target sites using a newly constructed optimization model of the transmitter currents and a matching control strategy. Stable and synchronized transmitter currents are achieved using a double-resonant circuit architecture with LCC correction. Also, cross-coupling will not be an issue for multiinput WPT systems anymore. A single controller and a direct current power source are all that's needed to provide full-range magnitude control. Under weak coupling conditions, the switching frequency may be decreased and system efficiency can be enhanced by employing the hybrid frequency pacing technique. Modeling and experimental findings using a real wireless rechargeable medical implant as the study object have confirmed the system's viability and potential.

**Xiaoyang Tian et al [2022]** offers new On the receiving end of a wireless power transfer (WPT) system, a bridgeless rectifier based on Cuk is suggested. In addition to contributing to greater overall efficiency, the suggested converter has a large power modulation range and little output current ripple. The suggested single-stage converter combines a bridgeless rectifier with a Cuk converter, with the input inductor of the latter being reduced, in order to meet the requirements of a series-series-compensated WPT system for output current source characteristics. In addition, the suggested converter's synchronization operation technique is developed to achieve the most efficient and effective operating point for transmission power. We take a look at the converter's inner workings and how they affect the efficiency of the WPT system. There are also provided design approaches for the system's parameters. In order to ensure that the suggested topology and operating mechanism are feasible, a prototype is constructed.

**Jialin Luo et al [2022]** The suggested single-stage converter is a hybrid of a bridgeless rectifier and a Cuk converter, with the input inductor of the latter being reduced. In addition, the suggested converter's synchronization operation technique is developed to achieve the most efficient and effective operating point for transmission power. We take a look at the converter's inner workings and how they affect the efficiency of the WPT system. There are also provided design approaches for the system's parameters. In order to ensure that the suggested topology and operating mechanism are feasible, a prototype is constructed. By modifying the duty cycle at various transfer distances and loads, the suggested converter is able to effectively alter the output power of the WPT system, allowing it to achieve the ideal operating point.

**Yanwei Jiang et al [2020]** is based on a fractional-order resonant circuit that uses just a fractional-order capacitor and suggests a fractional-order resonant WPT system. After the coupled-mode theory model of the proposed WPT system is developed, a research into the effects of various loads and orders on transfer quality is carried out. Assuming proper tuning of the fractional-order capacitor, theoretical studies show that the suggested system might provide a load-independent, constant current output. The experimental findings validate the theoretical analysis while developing the prototype of the fractional-order resonant WPT system.

**Zhengrong Huang et al [2020]** A method for reducing switching loss in three-phase PV inverters working under unity and nonunity power factor scenarios is suggested, which is based on critical-conduction-mode soft-switching modulation. The suggested improvements allow zero-voltage-switch turn-on or valley drain-source voltage turn-on for the typical power factor range of 0.8 lagging condition to 0.8 leading condition in PV applications, which is a huge boon for systems based on silicon carbide (SiC) that run at high switching frequencies and aim for high power density and efficiency. A single inexpensive microcontroller is used to digitally implement the suggested modulation method. Soft switching in nonunity power factor circumstances is achieved using a prototype three-phase bidirectional ac-dc converter based on SiC metal. Reactive power transmission capabilities and the advantages of enhanced modulation are experimentally verified.

**Indla Rajitha Sai Priyamvada et al [2022]** suggests ways for adaptively adjusting PV control settings using Lyapunov function analysis to raise the stability-limited power transfer capacity limit of transmission lines linking PV generators to the grid. Both the inner and outer control loop parameters, in addition to the PLL, are included in the suggested tuning recommendations. The suggested tuning concepts are basic fault-tolerant and will hold true regardless of changes to the system's topology, generation, loads, network impedances, or sun irradiation. We use an IEEE-118 bus system, a modified IEEE-39 bus system, and a Single PV-Synchronous Machine system to evaluate the method's performance. Transmission line failures (both symmetrical and asymmetrical), switching of transmission lines, fluctuations in PV solar irradiation, and other disturbances are all taken into account while analyzing the efficiency of the suggested system. The suggested tuning approach outperforms the current methodology in terms of stability and maximum power transfer capacity.

**Sachin Jain et al [2021]** suggested a method that, using data on the load voltage, allows for the seamless transition between modes. It prolongs the battery's life by preventing the switching cycle's charging and discharging phases from overlapping. Furthermore, the power information and complicated calculations (such as division, etc.) are not necessary for the functioning of the provided control method. Maximum power point tracking (MPPT) allows for autonomous management of the battery's charging and discharging, making the provided solution simply implementable on any PV-battery-based hybrid system. In order to ensure the

functioning in several modes with smooth control, a simulation was conducted. Experimental data from the constructed lab prototype further justify the simulation results.

**Weiyang Zhou et al [2022]** proposes a fast and easy voltage-location global maximum power point tracking (VL-GMPPT) approach for PV arrays operating under GLBC conditions, with the goal of minimizing the voltage searching range. To accomplish this, a GLBC-based mathematical model of the global maximum power point (GMPP) of a PV array is constructed. After that, the VL-GMPPT technique uses the IncCond approach to precisely locate the GMPP and a voltage-location mechanism to immediately relocate the operating point to the area around the GMPP. The suggested GMPPT approach is validated by displaying the results of both experiments and simulations. It was discovered that the suggested approach may cut down on tracking time by 90% compared to the traditional global searching strategy.

**Fei Jiang et al [2022]** suggests a hybrid parallel compensator (IHPC) to increase the grid-connected inverter's power transfer performance for photovoltaic (PV) systems. To lower the dc-link voltage, a traditional inductive-coupling voltage source inverter is connected in series with a thyristor switched capacitor (TSC) module. Reducing the voltage stress on the insulated gate bipolar transistor (IGBT) and keeping the voltage resource inverter from losing power is possible when the dc-link voltage is low. In order to improve the power transmission capabilities of PV inverters, the first step is to examine the process of reactive compensation. Afterwards, the IHPC's circuit layout and operational philosophy are presented. Then, to fix the resonance issue brought on by the TSC linked in series with the L filter and enhance the IHPC's compensation performance, an ideal control method is suggested for the IHPC. Finally, experimental and simulation results confirm that the control approach and suggested IHPC work as intended.

**Liang-Rui Chen et al [2022]** In order to obtain a single-stage architecture, the string PV module is linked in parallel with the suggested BCSPD circuit. Consequently, a very efficient power discussion may be achieved. To address the current ripple issue, the current-injection mechanism is modified. Consequently, long-life film capacitors may be used in place of electrolytic capacitors, significantly reducing the necessary capacitance on the PV side. Furthermore, to fulfill the needs of real-world applications, the power regulation function is also achieved via the use of the battery storage system with droop control. In order to evaluate the system's efficiency, a 1200 W prototype was created and put into action. The suggested system is able to manage the load power situation, decrease current ripple, and monitor MPP, according to the experimental findings.

**Nirmal Mukundan Chakkamath Mukundan et al [2021]** As a result of lower switching frequency and higher efficiency, multilevel inverters are claimed to work at high power levels. The literature has described cascading H-bridge (CHB) multilevel inverters, which differ from conventional multilevel topologies in that they include a redundant structure. A trinary hybrid multilevel inverter produces the highest number of identical output voltage levels when the ratio of dc sources to CHBs is 1:3. This paper proposes a grid-connected solar power transfer system that uses trinary CHB multilevel inverters and modified second-order generalized integral control. Verifying the suggested system in a two-stage solar PV system involves using two CHB structures per phase and a single-input-multiple-output single-ended primary inductance converter. Grid synchronization and active power control are addressed by presenting a modified second-order generalized integral control. In order to provide balanced, sinusoidal, and unity power factor grid currents, the controller is intended to reduce dc-offset from the measured load currents.

**Chang Liu et al [2022]** suggests a way for modular differential power processing (mDPP) to turn photovoltaic (PV) panels into one another. Panels may be added or deleted from either series strings or paralleled connections using this modular technique. A control method that uses a voltage inner loop and a power outer loop monitors the maximum power point of each PV panel and converts only the differential power. Simplifying design, the suggested solution decouples the performance of each PV module's control loop. The accuracy of MPPT and the plug-and-play functionality of the PV system are both confirmed by the simulation results.

**Iam et al [2022]** suggests an IPT converter with one stage for charging batteries. While the transmitter helps reduce the modulated phase shift angle at the receiver side, improving efficiency, the receiver side directly regulates the output to comply with the CC/CV charging profile, all without feedback wireless communication and with a constant operating frequency. Both the stability and the cost of the hardware are improved when the transmitter and receiver do not communicate wirelessly. To further eliminate the need for an additional dc-dc converter, we further implicitly regulate the output voltage. Using a 1-KW charging station, we experimentally validate the suggested control mechanism, which achieves a peak efficiency of up to 94.35%.

**Zhi-Juan Liao et al [2021]** This work presents an MC-WPT system that is similar to electromagnetically induced transparency (EIT) and can keep its power and efficiency tolerable throughout a broad variety of transmission distances. First, the tri-coil MC-WPT system's circuit model is introduced, along with a number of important ideas, such as the EIT mechanism and Eigen parameters. Then, the EIT-like mechanism's parameter design conditions and the energy efficiency enhancement concept are established from an investigation of the system's Eigen state energy efficiency characteristics. To demonstrate the efficacy and precision of the suggested approach, real-world systems are then developed, modelled, and evaluated. The

suggested strategy significantly improves the effective transfer range when considering both output power and transfer efficiency, as shown by both the modeling and experimental findings. The technique shines when used to the construction of electric car charging heaps, which are the foundation for efficiently charging vehicles with varying chassis heights on the same pile.

### 3.EXISTING SYSTEM

Renewable energy sources (RESs) are becoming more important in distribution power systems to meet the rising energy demand and mitigate serious environmental pollutants. So, RESs are crucial because they supplement the non-renewable, high-energy-density sources that are harmful to the environment. Power generation from renewable sources, such as solar panels, wind turbines, biogas engines, etc., may be sourced via distributed RES. The widespread use of photovoltaic (PV) technology is a direct result of the abundant sun irradiation, setting it apart from the other RESs discussed before. Interconnection of the main power bus with loads and energy sources is made possible by the recent widespread adoption of a low voltage DC (LVDC) grid. This is necessary since most electronic devices only work on DC power and many distributed RESs generate energy in DC. In addition, the LVDC grid offers a potential solution to the issues with AC power grid's limits, such as a decrease in conversion costs, improved conversion efficiency, and the absence of difficulties with synchronization and stability. An illustration of a local energy exchange, including interconnect production, energy storage, and load consumption, is shown in Figure 3.1. But the LVDC grid can't function without centralized RES production, and this is what allows the LVDC grid to be improved in a sustainable fashion. In particular, a research found that fixing rooftop PV wiring problems may significantly cut labor costs—a major cost driver—by 30–40% and reducing the installation time to only one day. By cutting down on time, labor, and construction expenses, the suggested PV-IWPT system may have its installation cost decreased.

In addition to reducing post-maintenance costs, the drilling-free PV-IWPT system preserves building interiors from water damage and thermal discomfort caused by broken thermal bridges, which in turn renders the PV system inoperable. In addition, the system's overall performance will be impacted by the wire connection problem. There will be major maintenance headaches after installation if there is a wiring problem.

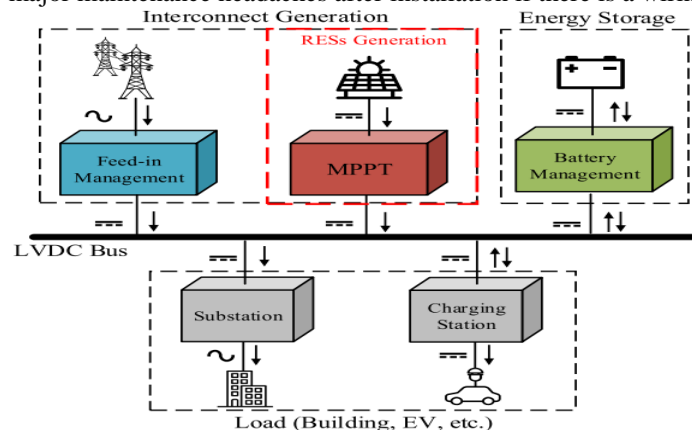


**Figure: 3.1** Schematic overview of a typical low-voltage DC grid

### 3.2 TEMPLATE SYSTEM STRUCTURE

Using a full bridge inverter on the transmitter side and a semi-active rectifier (SAR) on the receiver side, this study introduces and investigates a PV-driven single-stage series-series IWPT (SS-IWPT) converter, which bridges the gap in the PV-IWPT system (Figure 3.2). The amount of power that the PV array is able to produce is dependent on the input resistance of the IWPT converter. With a constant operating frequency, the PV's MPPT is implemented by the inverter on the transmitter side. We use a hybrid algorithm that combines particle swarm optimization (PSO) with auxiliary Perturb and Observe (P&O) to achieve the global maximum power point (MPP) of the PV array. This allows us to test the system's feasibility in different irradiance conditions, including rainy ones.

There is no need for wireless feedback communication between the transmitter and receiver sides since the maximum transmission efficiency is maintained exclusively by the receiver-side SAR using phase-shift pulse width modulation (PWM). The actual thickness of the roof wood is also taken into account by the transfer distance.

This study provides a brief overview of the PV-IWPT system's characteristics and its contributions:

- Less wire required and no drilling means cheaper installation
- Minimizes maintenance costs by preventing temperature discomfort and water penetration.

Single-stage SS-IWPT converters have inherent isolation properties, reduce system size and cost, and achieve high overall efficiency by simultaneously achieving MPPT of the PV array and MEPT of the whole PV-IWPT converter system. This is something that current PV-IWPT systems don't take into account. They also work well in a variety of shading conditions and even when it's raining. Operating the PV-IWPT at a set frequency eliminates the demand for feedback wireless transmission.

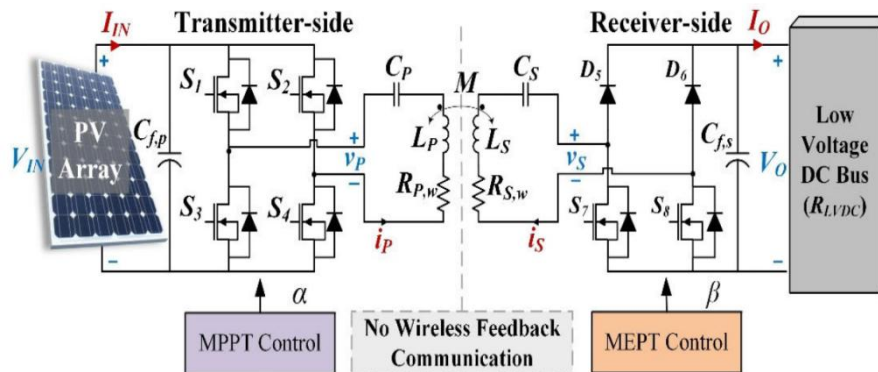


**Figure: 3.2** Circuit configuration of the proposed PV-IWPT system and its control scheme

The suggested PV-IWPT system is shown in Figure 3.2. The PV array is located at the transmitter side and drives the SS-IWPT. At the reception side, the SAR is used to optimize efficiency directly. There are three inductances shown in the PV-IWPT converter schematic: M, LP, and LS, which are self-inductances. Two diodes, D5 and D6, make up the upper legs of the SAR, which receives the input voltage  $v_S$  and current  $i_S$  from the two MOSFET switches, S7 and S8, which are located in the bottom legs. The SAR is linked in parallel with a large output capacitor,  $C_{f,s}$ . The PV-IWPT converter's dc output voltage is  $V_O$ , while its current output is  $I_O$ . The voltage of the LVDC bus should match the value of  $V_O$  because the PV-IWPT system's output is connected to it.

#### DRAWBACKS OF EXISTING SYSTEM

Problems with implementation, tuning, and real-time operation resulted from the control strategy's increased complexity caused by integrating particle swarm optimization with an auxiliary Perturb and Observe (P&O) method.

- The system's overall efficiency is reduced due to scalability issues;
- The system's capacity to dynamically adapt to changing circumstances may be limited in the absence of wireless feedback communication.
- How well PSO works with the P & O method, which is condition and parameter sensitive. Frequent modifications and fine-tuning are necessary due to the impact of changing environmental conditions or system components on performance.

### 4.PROPOSED SYSTEM

#### 4.1 PROPOSED SYSTEM BLOCK DIAGRAM

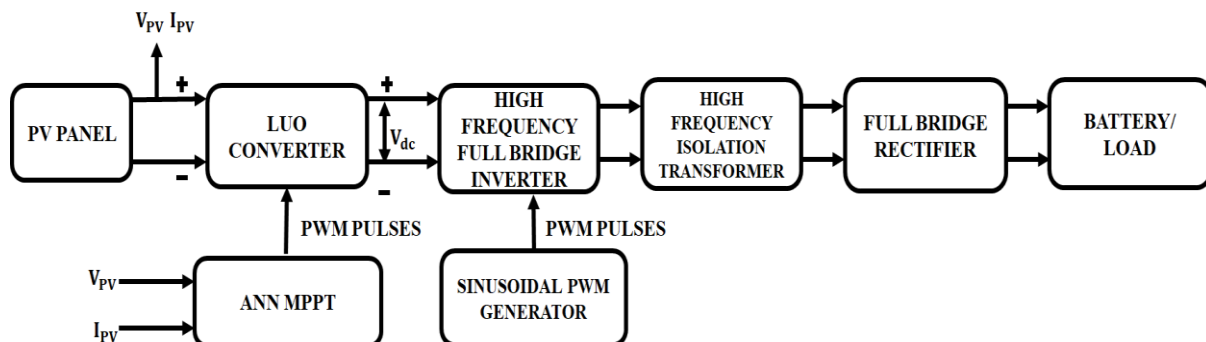


**Figure: 4.1** Proposed Block diagram

Rooftop photovoltaic (PV) systems are planned to be used in this system to generate electricity. One renewable and decentralized energy source is photovoltaic (PV) panels, which convert sunlight into direct current (DC) power. The Maximum Power Point Tracking (MPPT) technique, which is based on Artificial Neural Networks (ANNs), is used to maximize the power extraction from the PV panels. This smart algorithm adjusts to different weather conditions, figuring out how to make the PV system work as efficiently as possible even while partially shaded. The Luo converter improves the efficiency and performance of the energy conversion process by precisely monitoring and optimizing the power output from the PV panels. After that, a high-frequency converter receives the signal from the Luo converter. With this part, wireless power transmission

is possible, therefore wires aren't needed for the transfer of energy. Thanks to this wireless function, the system becomes more versatile and scalable, making it ideal for a range of uses. Connecting the high-frequency converter's output to an isolation transformer guarantees safety and dependability. The high-frequency converter is isolated from downstream components by this transformer, which protects the system as a whole from electrical risks. After the transformer's isolated output is directed towards an EV-specific battery, the system is ready for use. This battery stores the extra power from the PV system and uses it later. Also, DC loads may be fed the stored energy, so there's a constant supply of power for all sorts of things.

#### 4.2 LUO CONVERTER

A LUO converter is used to increase the voltage that is obtained from PV and wind. With its great efficiency and minimal ripples, this converter reaches a maximum output voltage. You can see the circuitry of the LUO converter in Figure 4.5. The components of this circuit are a switch (S), a diode (D), a coupling capacitance (C<sub>1</sub>) that stores energy, an inductance (L<sub>1</sub>) that transmits energy from the input side to the output side, and a low-pass filter (L<sub>2</sub>) and a capacitance (C<sub>2</sub>).

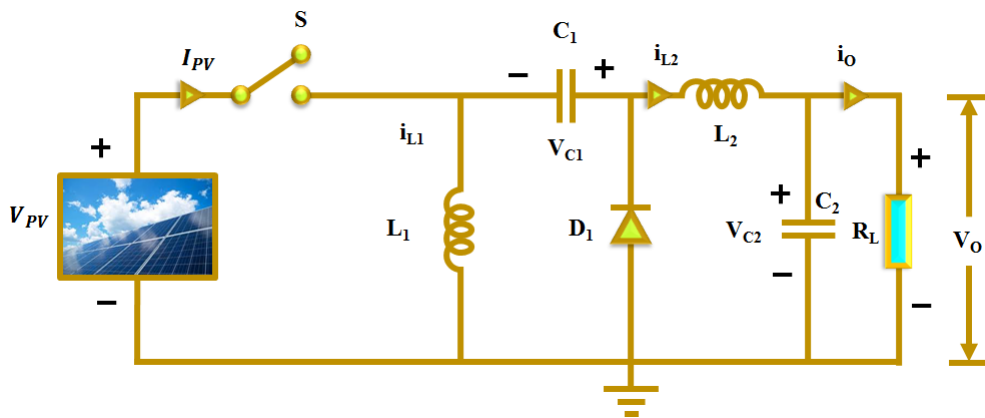


Figure: 4.2 LUO converter's circuit

Depending on the current passing through inductance L<sub>1</sub>, it does not function in either Continuous Conduction Mode (CCM) or Discontinuous Conduction Mode (DCM). The operation of CCM is taken into account in this study.

#### 4.2.1 Modes of Operation of LUO converter

Two switching modes such as closed and open states are required when analysing the LUO converter's working principle.

##### Mode 1

The LUO converter's circuit layout of mode 1 is displayed in Figure 4.2.1.1.

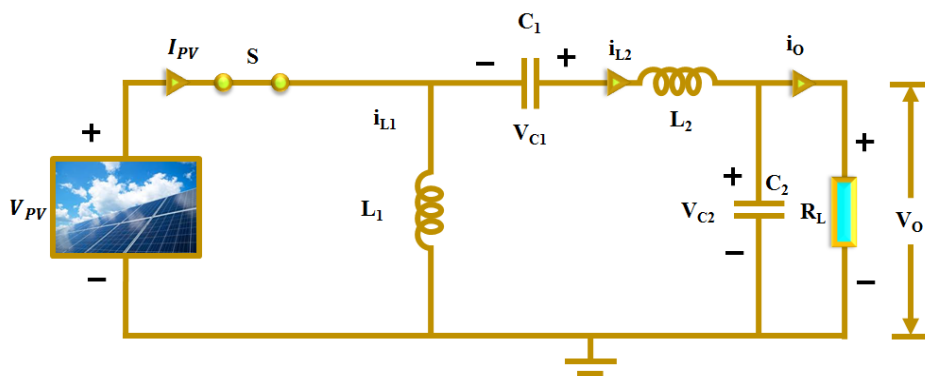
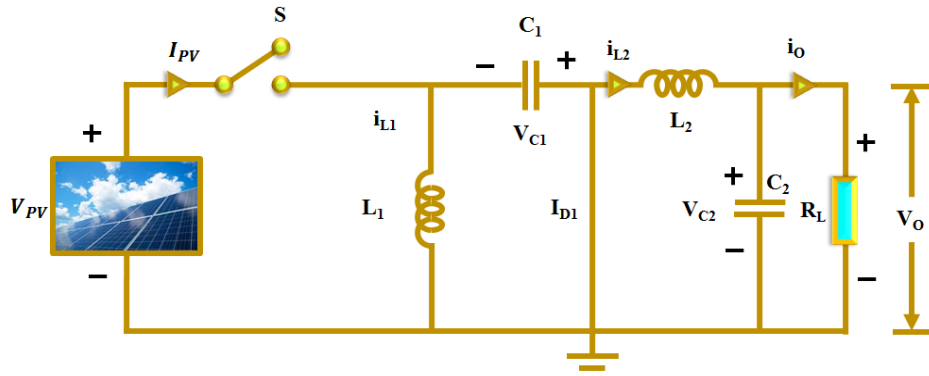


Figure: 4.2.1.1 Mode 1

Under these conditions, the diode (D) is reverse biased and the switch (S) is closed. In this state, the input PV current ( $i_{PV}$ ) is equal to the sum of the inductive currents ( $i_{L_1}$ ) and ( $i_{L_2}$ ), while the input PV voltage charges the inductance (L<sub>1</sub>). During this time, the input photovoltaic (PV) energy is absorbed by the capacitance (C<sub>1</sub>) and inductance (L<sub>2</sub>), leading to a rise in inductive currents ( $i_{L_1}$ ) and ( $i_{L_2}$ ).

##### Mode 2

The LUO converter's circuit layout of mode 2 is displayed in Figure 4.2.1.2.



**Figure: 4.2.1.2 Mode 2**

Here, we have a forward biased diode and an open switch (S). In this mode, the input PV current is zero and the capacitance ( $C_1$ ) is charged by the inductive current ( $i_{L1}$ ) flowing through the diode (D). At the same time, the inductive current ( $i_{L2}$ ) drops because it goes through the capacitance ( $C_2$ ) and the resistive load ( $R_L$ ). In this case, the inductive currents become  $i_{L1} \neq I_{L1}$  and  $i_{L2} \neq I_{L2}$ , where  $I_{L1}$  and  $I_{L2}$  are the mean inductive currents that flow through  $L_1$  and  $L_2$ , respectively, and the variances in these currents are less.

During open condition, the charge on capacitance  $C_1$  increases. It is expressed as,

$$Q_+ = (1 - D)I_{L1} \quad (4.16)$$

During closed condition, the charge on capacitance  $C_1$  decreases. It is expressed as,

$$Q_- = DI_{L2} \quad (4.17)$$

Where the duty cycle of switch (S) is specified as  $D = \frac{T_{on}}{T}$ ,

In an entire cycle,  $Q_+ = Q_-$ , by utilizing this relation, the inductive current  $I_{L2}$  is derived. It is expressed as,

$$I_{L2} = \frac{1-D}{D} I_{L1} \quad (4.18)$$

Because the capacitance ( $C_2$ ) acts as a LPF, the current output ( $I_0$ ) is specified in equation (4.19).

$$I_{L2} = I_0 \quad (4.19)$$

During closed condition, the input PV current is specified as  $i_{PV} = I_{L1} + I_{L2}$ , whereas during open condition  $i_{PV} = 0$ . As a result, the average input PV current  $I_{PV}$  is expressed as,

$$I_{PV} = D * i_{PV} = D(I_{L1} + I_{L2}) = D \left(1 + \frac{1-D}{D}\right) I_{L1} = I_{L1} \quad (4.20)$$

The output current ( $I_0$ ) is expressed as,

$$I_0 = \frac{1-D}{D} I_{PV} \quad (4.21)$$

The output voltage ( $V_0$ ) is expressed as,

$$V_0 = \frac{D}{1-D} V_{PV} \quad (4.22)$$

Where  $V_0$  is the output voltage and  $I_0$  is the output current. In both the open and closed states, Table 4.1 shows the instantaneous currents and voltages of the inductance (L) and capacitance (C).

**Table: 4.1** Current and voltage in L and C during switch ON and OFF state

<b>Voltage /Current of <math>L</math> &amp; <math>C</math></b>	<b>During closed condition of switch <math>0 &lt; t &lt; DT</math></b>	<b>During opened condition of switch <math>DT &lt; t &lt; T</math></b>
$V_{SW}$	0	$V_0 + V_{PV}$
$V_{L_1}$	$V_{PV}$	$-V_0$
$V_{L_2}$	$V_{PV}$	$-V_0$
$i_{L_1}$	$i_{L_1}(0) + \frac{V_{PV}}{L_1} t$	$i_{L_1}(DT) + \frac{V_0}{L_1} (t - DT)$
$i_{L_2}$	$i_{L_2}(0) + \frac{V_{PV}}{L_2} t$	$i_{L_2}(DT) - \frac{V_0}{L_2} (t - DT)$
$i_{C_1}$	$i_{L_2}(0) + \frac{V_{PV}}{L_2} t$	$-i_{L_1}(DT) - \frac{V_0}{L_1} (t - DT)$
$i_{C_2}$	$i_{L_2}(0) + \frac{V_{PV}}{L_1} t - I_0$	$-i_{L_1}(DT) - \frac{V_0}{L_1} (t - DT) - I_0$
$V_D$	$V_{PV} + V_0$	0

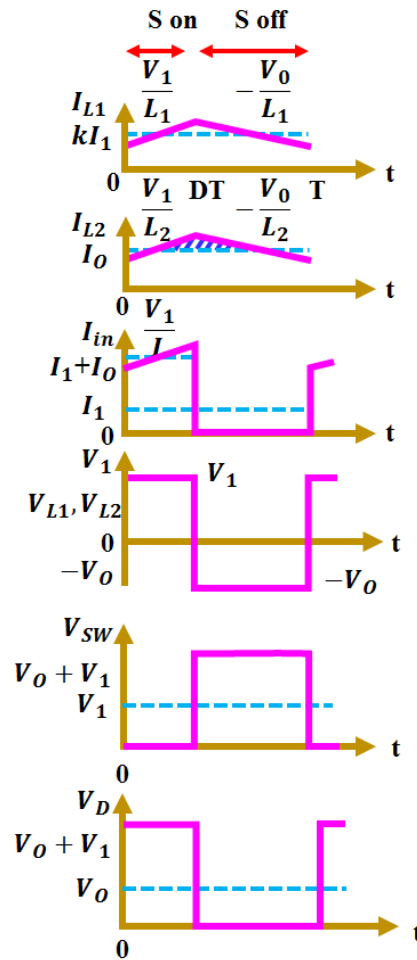


**Figure: 4.2.1.3** Waveforms of LUO converter

The voltage and current waveforms of LUO converter for various modes are displayed in Figure 4.2.1.3.

### 4.3 ANN BASED MPPT

We provide a novel ANN-based MPPT approach for monitoring the maximum power output of PV modules in response to dynamic weather circumstances. All three of these parameters—PV voltage,  $I_{pv}$  current, and  $T_{pv}$  cell temperature—are suggested as inputs. The duty cycle serves as the output variable that regulates the DC-DC switching boost Landsman converter, ensuring that maximum power is continuously tracked. The likelihood of attaining optimum performance is limited due to the fact that standard FLC modeling relies on trial and error. Consequently, acquiring artificial neural networks provides an other approach to dealing with nonlinear issues. They are able to handle partial data and learn from examples. They are able to make quick predictions after training. Every measurement of irradiance and temperature has its own unique maximum power point (MPP) in the PV module. To find this MPP, the output of the PV module must be applied with the voltage that corresponds to it,  $V_{mp}$ .

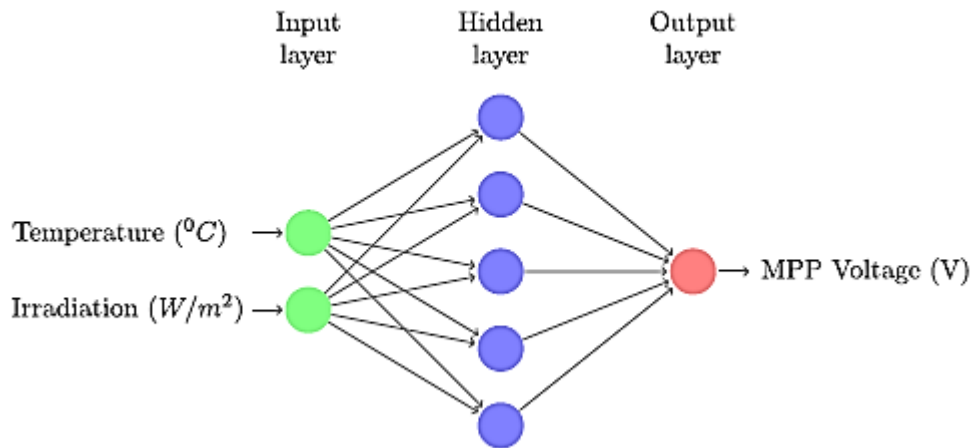


**Figure: 4.3** Structure of ANN

As seen in Figure 4.3, the proposed ANN-based MPPT controller is built using a two-layer feed-forward network. Layers, neuron densities, activation functions, and interconnections between them all contribute to the overall structure of a neural network. To improve the accuracy of the neural network that is produced, this structure is selected after several experiments. The two neurons in the input layer are responsible for transmitting the irradiance and temperature to the hidden layer. Five neurons with hyperbolic tangent activation functions make up the hidden layer. The weight matrix (WH) and biases vector (bh, bo) describe the intensities of the neurons in the hidden and output layers, respectively. Both the temperature (T) and the irradiance (G) are included in the input signal vector. The estimated MPP voltage  $V_{mp}$  is provided by one neuron in the output layer, which has a linear activation function. In order to train the neural network with accurate predictions, the database should include many different types of metrics. We minimize the mean square error (MSE) using the approximation Hessian matrix during the offline training of the neural network using the Levenberg-Marquardt back propagation technique. Due to its shown processing efficiency and outstanding performance, this method is selected as the optimization tool. The validation MSE curve is quite close to the training MSE curve, which means the ANN learning was successful. The MPP voltage should be provided by the ANN-based MPPT controller under any weather situation after training. This controller has the benefit of not requiring a large number of iterations to find the MPP. This enhances the controller's performance and decreases oscillations around the MPP. Incorporating a calculator into this method makes us realize that irradiance and temperature sensors are necessary.

#### 4.4 HIGH FREQUENCY INVERTER

Electrical circuits that transform low-frequency direct current (DC) into high-frequency alternating current (AC) are known as high-frequency inverters. The output waveform's frequency usually falls anywhere between a few kilohertz and a few megahertz. Induction heating, electric car motor drives, and power supply for electronic devices are just a few of the many popular uses for high frequency inverters. A high frequency inverter typically has a rectified AC voltage or DC input source, a power transistor or an IGBT for high frequency switching, and a transformer or LC circuit for resonance circuitry.

A high-frequency switching device is used to generate an alternating current (AC) waveform by rapidly turning the DC input voltage on and off. Matching the output impedance to the load and shaping and amplifying the AC waveform are both accomplished by use of the resonant circuit.

### 5.RESULTS AND DISCUSSIONS

#### 5.1 RESULT VIEW

The proposed work is implemented in MATLAB simulation and the following results are obtained.

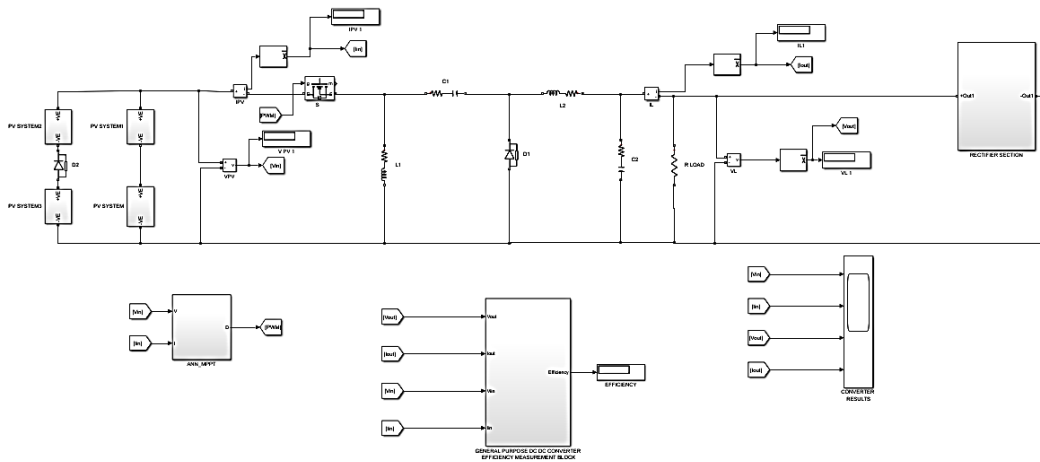


**Figure: 5.1** over allSimulation Diagram

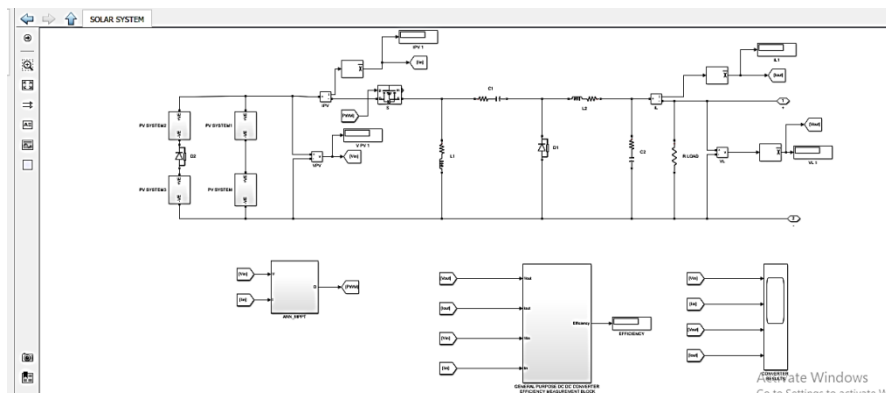


**Figure: 5.2** Simulation Diagram for solar with Luo converter

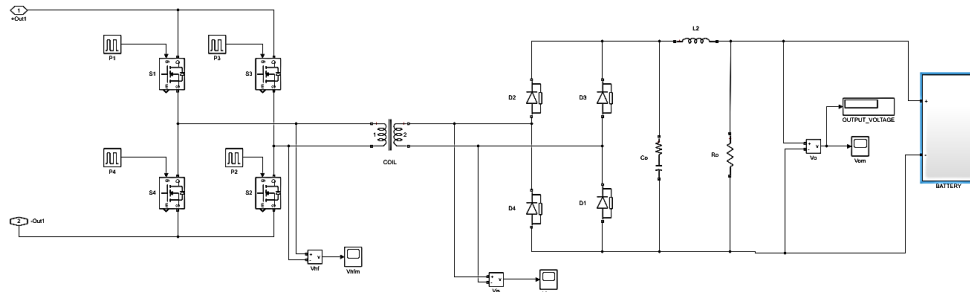


**Figure 5.3** Simulation Diagram for Rectifier section

**CASE (1)  
 UNDER PARTIALLY SHADED CONDITION**

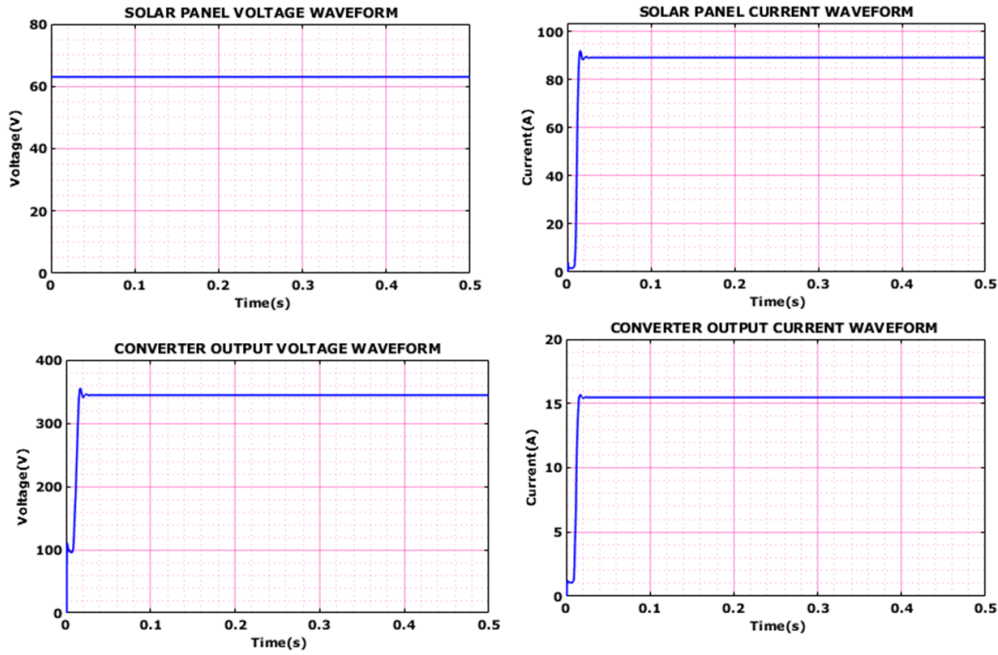


**Figure: 5.4 (a)** under shaded condition

Figure 5.4 (a) shows the voltage waveform of solar panels while partly shaded. The output voltage waveform under partly shadowed conditions is shown in figure 5.4 (a). The LUO converter receives an input voltage of 64V when partly shaded. The potential voltage at the output can be close to 350V. It monitors the PV panel's maximum power output using an ANN mppt algorithm. The suggested converter ensures a consistent and sustained output voltage.

**CASE (2) UNDER NORMAL CONDITION**

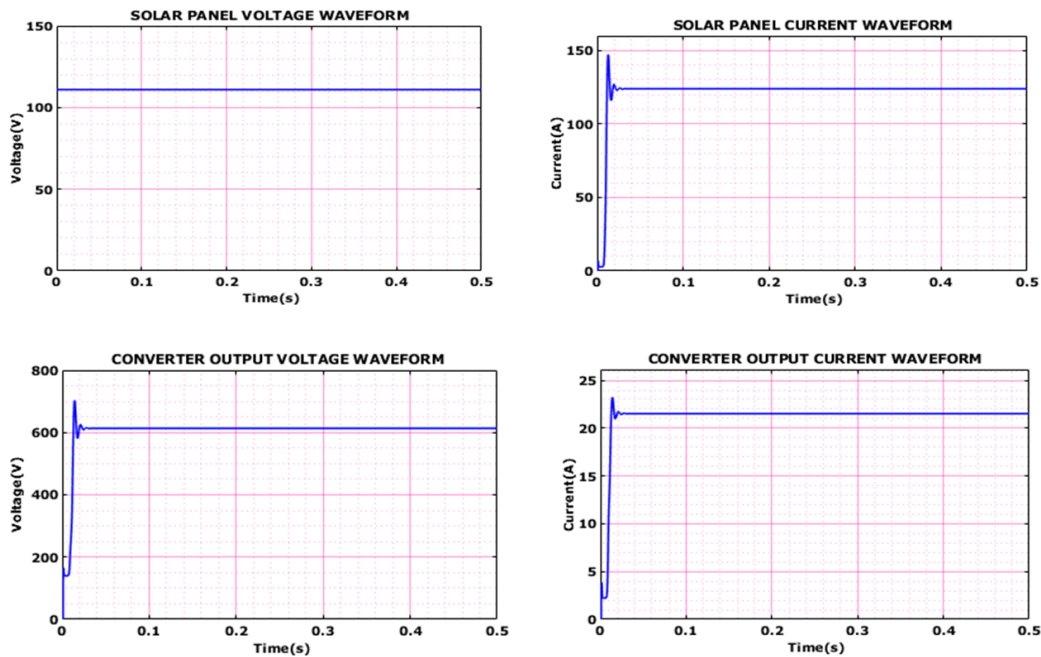


**Figure: 5.5 (a)** Under Normal operating condition

Figure 5.5 (a) shows the voltage waveform of the solar panels while they are running normally. Under typical working conditions, the waveform of the output voltage is shown in figure 5.5 (a). To create a partly shadowed area, you may reduce the power output of two or three of the almost 700 PV panels. The LUO converter is now receiving a 64V input voltage in partly shaded conditions. The potential voltage at the output can be close to 350V. It monitors the PV panel's maximum power output using an ANN mppt algorithm. The suggested converter ensures a consistent and sustained output voltage.

Drawing conclusions about converter efficiency, we find that it is close to 90% in both situations 1 and 2. A

steady output voltage is maintained by the suggested converter, and the maximum power is tracked by the proposed ANN controller.

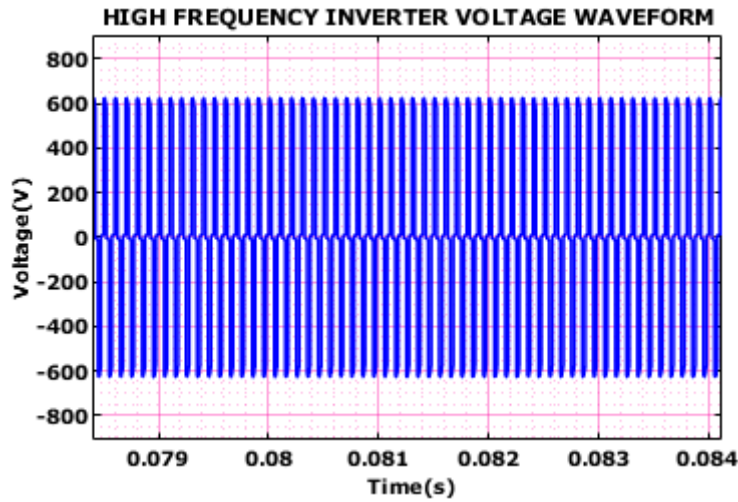


Figure: 5.6 High frequency inverter voltage waveform

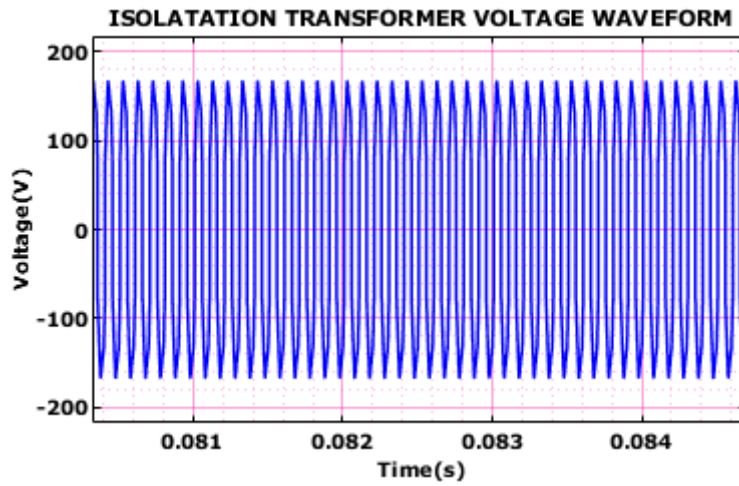


Figure: 5.7 Isolation Transformer Output Voltage waveform

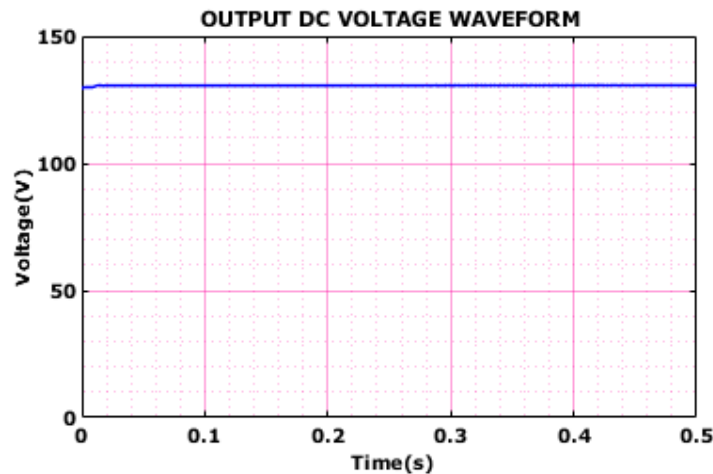
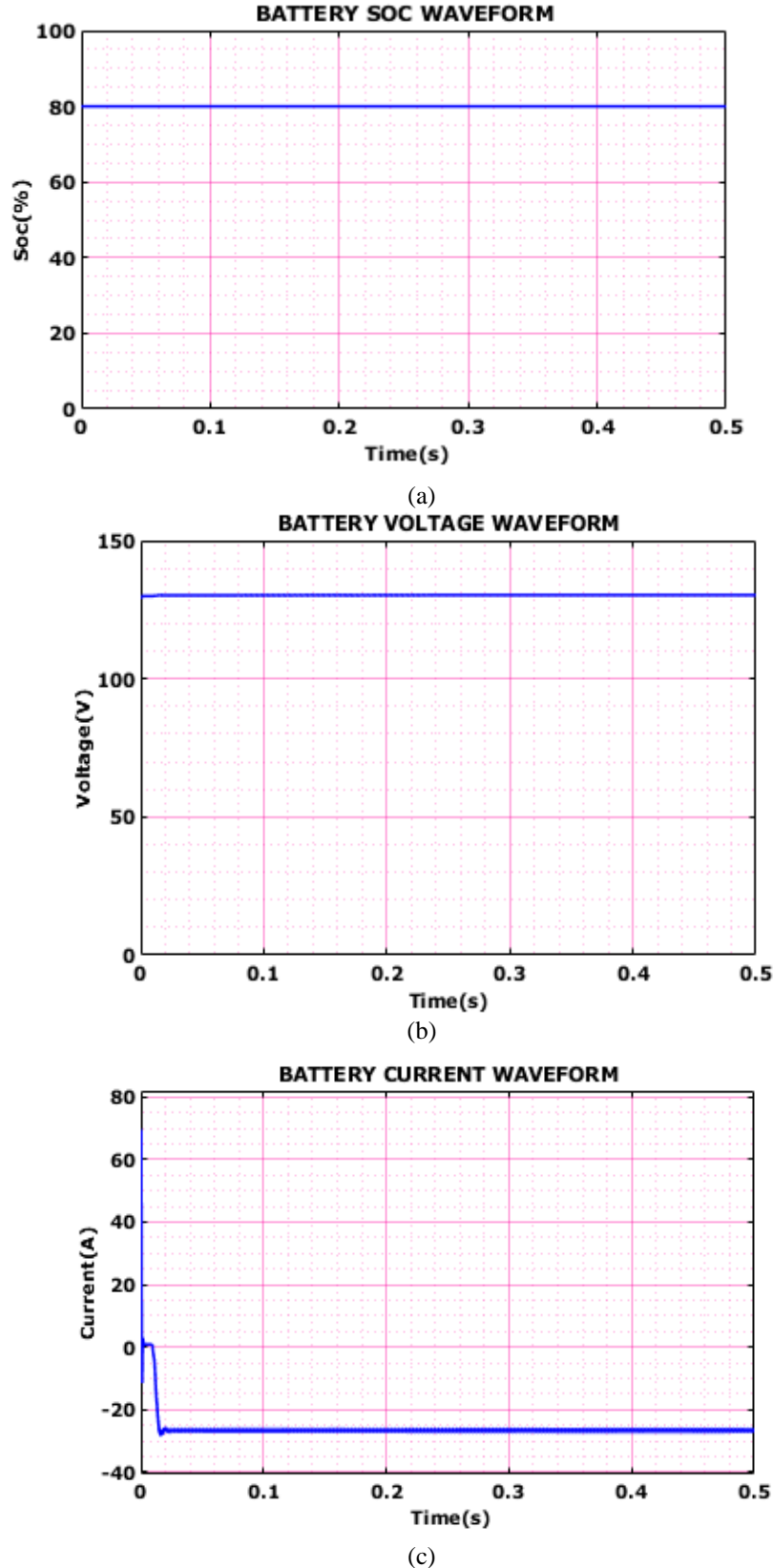


Figure: 5.8 Rectifier output voltage waveform

The Figure 5.8 Forward Converter represent the waveform for dc load which provide galvanic isolation in figure 5.7 for protection. The 130V produced from the converter is given to DC load as battery.



**Figure: 5.9** Waveforms of battery (a) SOC and (b) Voltage (c) Current

Figure 5.9 shows the waveforms that reflect the voltage and state of charge of the battery. The voltage of the batteries is 120V. As shown in Figure 5.9 (b), the waveforms for the state of charge (SOC) of the battery are successfully monitored, and it is 80%. Using batteries, the excess electricity that is produced by the PV is stored. In the event that the main power source is down, the backup battery will deplete and provide electricity to the load.

## CONCLUSION

Ultimately, this study presents a novel method for using PV systems on rooftops for centralized generation inside low-voltage (LV) DC networks that is linked with buildings. Overall power production efficiency is improved by using an ANN MPPT algorithm, which guarantees optimum power extraction from the PV panels, particularly in partly shadowed situations. The next step in wireless power transfer is to direct the energy into a high-frequency converter. Not only does this wireless transmission capability allow for smooth energy transfer, but it also makes the system more adaptable and scalable by doing away with physical connections. Connecting the high-frequency converter's output to an isolation transformer strengthens the system's dependability and safety. At the same time as DC loads are being powered, the separated output of the transformer is being directed towards an electric vehicle (EV) battery. There is a rising need for sustainable energy solutions for both fixed and mobile applications, and this dual capability boosts the system's adaptability. We will do a battery of numerical simulations in MATLAB 2021a/Simulink to make sure the controls and system design we're proposing work.

## FUTURE SCOPE

- Energy storage systems: increase the dependability of stand-alone load systems by integrating PI controllers with energy storage devices like batteries or supercapacitors. Its primary function was to regulate the energy stored in such systems, maintaining a steady flow of electricity to the load.

- Advancements in affordable system design and manufacturing: Communities requiring dependable and long-term stand-alone load solutions will be able to afford PI controllers in the future.

Interleaved converter performance may be improved by the use of sophisticated control algorithms. These methods can include adaptive control and model predictive control (MPC). Better control precision and stability may be achieved by enhancing the converter's reaction to variations in input voltage or load demand using these techniques. Connected devices would completely alter the way electric vehicles are charged. To improve charging experiences and make the most efficient use of resources, it will intelligently link grids, networks, renewable energy, batteries, and vehicles. The term "Internet of Vehicles" (IoV) would describe this setup. There will be a dramatic uptick in the market for battery-powered transportation vehicles. Large corporations want to project an image of being ecologically conscious. Deploying zero-emission commercial cars is a part of their present plan. That is why EV charging companies will have to build mega-chargers to make these massive EVs usable over longer distances.

The equipment that was created has been tested on a small scale in the lab, and it may be safely installed in my substations to ensure that it works as intended in a real-world setting. If the load is dynamic, automated PF correction could lead to harmonic problems due to the bank of capacitors being switched on and off so often. To prevent the frequent switching of capacitor banks, it is possible to build an optimal algorithm and a suitable filter based on the frequent load change pattern. It is possible to do a comparison analysis to determine the best spot for correctional equipment in terms of efficiency and cost-effectiveness in the field.

## REFERENCES

1. Weiyang Zhou;Ke Jin;Ran Zhang, Year:2022, "A Fast-Speed GMPPT Method for PV Array Under Gaussian Laser Beam Condition in Wireless Power Transfer Application", IEEE Transactions on power Electronics, vol.37, no.8, pp.10016 – 10028.
2. Aranzazu D. Martin;J. M. Cano;J. Medina-García;J. A. Gómez-Galán;Jesus R. Vazquez, Year:2020, "Centralized MPPT Controller System of PV Modules by a Wireless Sensor Network", IEEE Access, vol.8, no.71694 – 71707.
3. Xujian Shu; Bo Zhang; Zhihao Wei; Chao Rong; Shubin Sun, Year:2021, "Extended-Distance Wireless Power Transfer System With Constant Output Power and Transfer Efficiency Based on Parity-Time-Symmetric Principle", IEEE Transactions on Power Electronics, vol.36, no.8, pp.8861 – 8871.
4. Huanjie Zhu; Bo Zhang; Lihao Wu, Year: 2020, "Output Power Stabilization for Wireless Power Transfer System Employing Primary-Side-Only Control", IEEE Access, vol.8, no.63735 – 63747.
5. Fandan Zhao; Jinhai Jiang; Shumei Cui; Xingjian Zhou; Chunbo Zhu; Ching Chuen Chan, Year:2022, "Research on Bipolar Nonsalient Pole Transmitter for High-Power EV Dynamic Wireless Power Transfer System", IEEE Transactions on Power Electronics, vol.37, no.2, pp.2404 – 2412.
6. Jialong Qu; Liangxi He; Niang Tang; Chi-Kwan Lee, Year:2020, "Wireless Power Transfer Using Domino-Resonator for 110-kV Power Grid Online Monitoring Equipment", IEEE Transactions on Power Electronics, vol.35, no.11, pp.11380 – 11390.
7. Lihao Wu; Bo Zhang; Jiali Zhou, Year:2020, "Efficiency Improvement of the Parity-Time-Symmetric Wireless Power Transfer System for Electric Vehicle Charging", IEEE Transactions on Power Electronics, vol.35, no.11, pp.12497 – 12508.

8. Xiaoyang Tian; Kwok Tong Chau; Wei Liu; Hongliang Pang; Christopher H. T. Lee, Year:2022, "Maximum Power Tracking for Magnetic Field Editing-Based Omnidirectional Wireless Power Transfer", IEEE Transactions on Power Electronics, vol.37, no.10, pp. 2533 – 254.
9. Jialin Luo; Wenxun Xiao; Guidong Zhang; Dongyuan Qiu; Bo Zhang; Fan Xie; Yanfeng Chen, Year:2022, "Novel Cuk-Based Bridgeless Rectifier of Wireless Power Transfer System With Wide Power Modulation Range and Low Current Ripple", IEEE Transactions on Industrial Electronics, vol.69, no.3, pp.2533 – 2544.
10. Yanwei Jiang; Bo Zhang; Jiali Zhou, Year: 2020, "A Fractional-Order Resonant Wireless Power Transfer System with Inherently Constant Current Output", IEEE Access, vol.8, pp.23317 – 23323.
11. Zhengrong Huang; Qiang Li; Fred C. Lee, Year:2020, "Critical-Conduction-Mode-Based Soft-Switching Modulation for Three-Phase PV Inverters With Reactive Power Transfer Capability", IEEE Transactions on Power Electronics, vol.35, no.6, pp.5702 – 5713.
12. Indla Rajitha Sai Priyamvada; Sarasij Das, Year: 2022, "Adaptive Tuning of PV Generator Control to Improve Stability Constrained Power Transfer Capability Limit", IEEE Transactions on Power Systems, vol.37, no.3, pp. 1770 – 1781.
13. Sachin Jain; Sumon Dhara; Vivek Agarwal, Year:2021, "A Voltage-Zone Based Power Management Scheme With Seamless Power Transfer Between PV-Battery for OFF-Grid Stand-Alone System", IEEE Transactions on Industry Applications, vol.57, no.1, pp. 754 – 763.
14. Weiyang Zhou; Ke Jin; Ran Zhang , Year:2022, "A Fast-Speed GMPPT Method for PV Array Under Gaussian Laser Beam Condition in Wireless Power Transfer Application", IEEE Transactions on Power Electronics, vol.37, no.8, pp.10016 – 10028.
15. Fei Jiang; Xing Peng; Chunming Tu; Qi Guo; Jie Deng; Fengzhe Dai, Year:2022, "An Improved Hybrid Parallel Compensator for Enhancing PV Power Transfer Capability", IEEE Transactions on Industrial Electronics, vol.69, no.11, pp.11132 – 11143.
16. Liang-Rui Chen; Chia-Hsuan Wu; Neng-Yi Chu; Cheng-Chih Chou; Fan-Jun Zheng, Year:2022, "Battery Current-Sharing Power Decoupling Method for Realizing a Single-Stage Hybrid PV System", IEEE Access, vol.10, pp.86864 – 86873.
17. Nirmal Mukundan Chakkamath Mukundan; Jayaprakash Pychadathil; Umashankar Subramaniam; Dhafer J. Almakhlles, Year:2021, "Trinary Hybrid Cascaded H-Bridge Multilevel Inverter-Based Grid-Connected Solar Power Transfer System Supporting Critical Load", IEEE Systems Journal, vol15, no.3, pp.4116 – 4125.
18. Chang Liu; Yue Zheng; Brad Lehman, Year:2022, "PV Panel to PV Panel Transfer Method for Modular Differential Power Processing", IEEE Transactions on Power Electronics, vol.37, no.4, pp.4764 – 4778.
19. Io-Wa Iam;Iok-U Hoi;Zhicong Huang;Cheng Gong;Chi-Seng Lam;Pui-In Mak;Rui Paulo Da Silva Martins, Year:2022, "Constant-frequency and noncommunication-based inductive power transfer converter for battery charging", IEEE Journal of Emerging and Selected Topics in Power Electronics, vol. 10, no. 2, pp. 2147–2162.
20. Zhi-Juan Liao; Qi-Kai Feng; Chen-Hui Jiang; Fan Wu; Chen-Yang Xia;Dong-Sheng Yu, Year:201, "Analysis and Design of EIT-Like Magnetic Coupling Wireless Power Transfer Systems", IEEE Transactions on Circuits and Systems I: Regular Papers, vol. 68, no. 7, pp. 3103–3113